Student Name	Orlando Andico	**HET615**	
Student ID	7170874	**Project Supervisor**	Mel Hulbert

SAO Project Cover Page

Project Title Low-Cost Encoder-Assisted Mount Tracking

16 November 2013

All of the work contained in this project is my own original work, unless otherwise clearly stated and referenced. I have read and understood the SAO Plagiarism Page "What is Plagiarism and How to Avoid It" at

http://astronomy.swin.edu.au/sao/students/plagiarism/

Overview

Astronomical imaging requires the capture of photons from the object of interest for a sufficient time to produce an acceptable signal-to-noise ratio. The use of tracking (a telescope mount which compensates for the Earth's rotation) is required for all but the shortest exposures and focal lengths (Covington, 1999). However, no cost-effective mechanical drive can rotate at precisely the required rate; there are always imperfections in the drive tracking due to unevenness in the gears which make up the drive. These imperfections cause the drive to speed up and slow down in a periodic or semi-periodic pattern with every rotation of the drive gears. This variation in tracking speed is called *periodic error* (Covington, 1999).

Lesser-quality telescope drives exhibit errors of magnitude 15" or more, while Covington notes that "exceptional" drives would exhibit errors of 5" or less. Compared to the Rayleigh resolution limit of 1" for a 140mm aperture instrument, a 5" *periodic error* is much larger and would drastically reduce the quality of observations made with such a mount. A perfectly polar-aligned mount would show no north-south drift (declination drift) but would exhibit east-west drift (star trailing) due to periodic error, as the telescope drive would alternately speed up and slow down due to mount imperfections. With greater magnitude of such periodic error would come greater elongation of stars (and the blurring of extended objects) in the captured image.

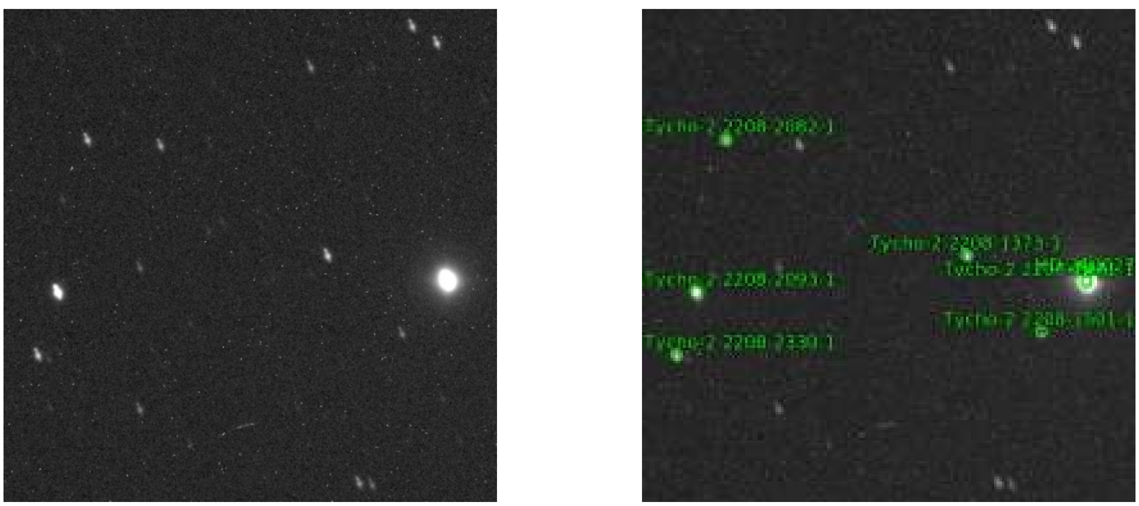

Fig. 1. Unguided 10-minute image of a 15' square region around RA 22h 07m 04.082s and DEC +25° 14' 36.712" exhibiting both north-south declination drift (left to right) and east-west drift due to periodic error (top to bottom)

The traditional method of dealing with periodic errors is *guiding*. Guiding can be done either manually or automatically. In both cases, a star is centered on a reticle or guide chip and *guide pulses* are used to speed up or slow down the telescope drive when the star deviates from the center of the reticle. This technique has been in use for at least 25 years (Reid, et al, 1991). The advent of inexpensive CCD detectors and computers has brought auto guiding within the reach of most amateur astronomers (Covington, 1999).

However, there are instances when guiding is not desirable or preferred – during periods of poor seeing or when observing star-poor regions of the sky; when the guiding CCD is behind a narrow-band filter; or when the guide star is purposely defocused to prevent saturating the CCD sensor in photometric studies (Colon and Gaidos, 2013). In these cases guiding may not be possible. There are also observation programs such as supernova and GRB searches which require multiple rapid slews (up to hundreds per night). With such observation programs, the necessity of acquiring a guide star, calibrating the guider, and waiting for the guider to settle are significant time overhead that cuts into actual observing time, for example Vanleenhove (2013).

An alternative approach for actively correcting the tracking and pointing of telescope mounts is the use of relative or absolute encoders on the Right Ascension and Declination (or Altitude and Azimuth) axes. Encoders potentially can provide much higher tracking resolution than guiding, which is limited by atmospheric seeing which perturbs the position of the guide star. The Gemini Mount Control System Report (1996) reported a requirement of 5 milli-arcseconds tracking resolution, which would be difficult to obtain with a guiding configuration.

Much of the early work on encoder-based tracking correction was done using alternating-current encoders called Inductosyns, also widely used for pointing radio telescopes such as the Very Large Array (Ruhle, 1996). Numerous studies have been done (e.g. Amos et al, 1992; Fisher, 1994) to characterize the performance of telescopes with Inductosyn or similar encoder technology. Fisher & Wilkes (1995, 1997) also conducted exhaustive comparisons (from a performance, accuracy, and cost perspective) of various encoder approaches.

The key challenge of encoder-based tracking correction, aside from cost, is that encoders have their own inherent errors – tape encoders exhibit their own periodic errors related to the lines on the tape, and rotary optical encoders exhibit periodic errors related to the subdivisions of the optical grating slots (Erm & Sandrock, 2002, 2005). Furthermore, physical disruptions such as sand or scratches on the encoder scales also induce errors (Gemini Mount Control System Report, 1996).

As Erm & Sandrock explain, errors in the encoders enter the servo loop, and at the low speeds of telescope drives, no position error would be detectable, but *the telescope would be moving with the error*. As early as 1984, Ulich et al (1984), The Gemini Mount Control System Report (1996), and Yang et al (2000) all reported significant reductions in encoder errors through the use of software techniques.

For example, the largest telescope in the Northern Hemisphere as of 2008, the Gran Telescopio Canarias, utilized a Heidenhain precision encoder with a published accuracy of 0.0003 arc-seconds. However systematic and other encoders resulted in a final system accuracy of 0.06 arc-seconds, a 200-fold reduction over the theoretical accuracy (HWeb, 2008).

Objectives

The aim of the project was to design and implement an encoder-based solution for correcting Right Ascension tracking errors (primarily due to periodic error) in an amateur-level mount. The goal was to obtain a tracking accuracy of within 4” peak-to-peak from a mount with a native periodic error in the 15” (peak-to-peak) range. Because telescope encoders have been in use for over 20 years, and amateurgrade encoders such as the Telescope Drive Master (Explore Scientific, 2013) are available at a cost to the end-user of approximately $2,000 (US), a further goal of the project was to create a design with a materials cost of under $500 (US). Such a goal would render the system practical and desirable to owners of mounts in the $1,000 to $2,000 (US) price range. Furthermore, the possibility of varying the tracking rate of the mount to match the refraction-corrected tracking rate and King rate was explored.

Methodology

A mechanism to couple an encoder disk to the Right Ascension axis of a typical German equatorial mount was fabricated. The mechanism used a machined shaft that threaded into the polar scope bore of the mount. Such a solution made the polar scope inaccessible; and further, on certain mount models the polar scope bore does not rotate with the RA axis – this approach would not be valid for these mounts. However the most common mounts which this project was intended for – e.g. the Orion Atlas or EQ6, Celestron CGEM, Losmandy G11 – all have rotating polar scope bores.

The encoder disk was constructed of acrylic plastic, with a 10mm channel machined into its circumference, 2mm in depth, in which a 2mm pole length Bogen magnetic tape was affixed using the self-adhesive backing of the tape. The Bogen magnetic tape had pole pairs spaced 2mm apart, and was of length 910mm giving approximately 1.424 arc-seconds per encoder tick. The encoder disk was 290mm in diameter. This could be compared to the length of the encoder track on the Gran Telescopio Canarias which was 48.48m (48480mm) or 53 times longer.

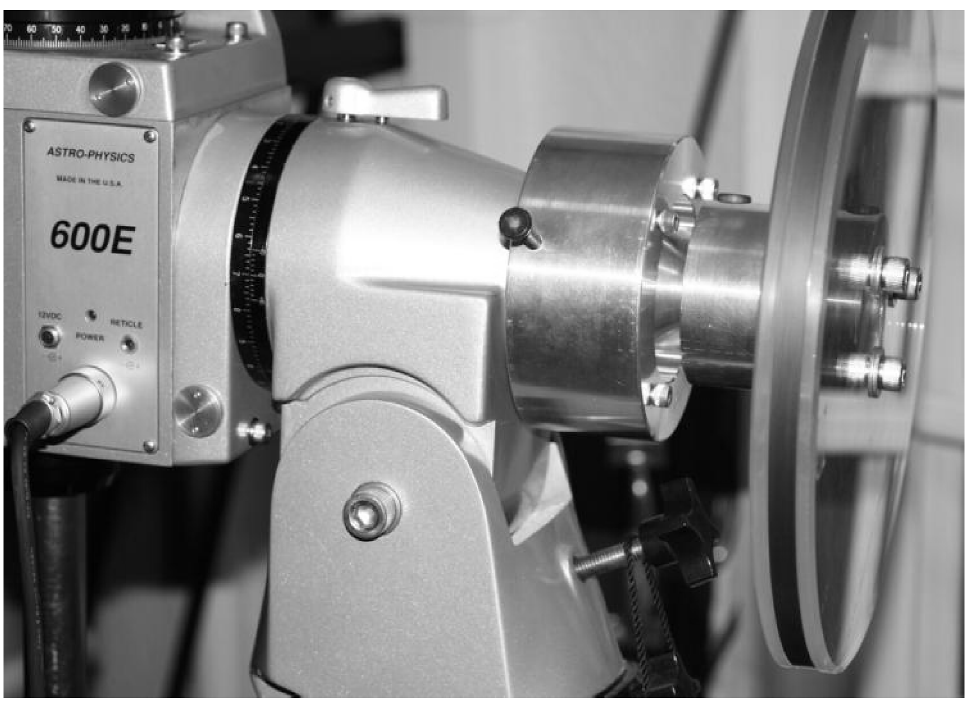

Fig. 2. Right Ascension shaft coupling, encoder read head mounting flange, and acrylic encoder disk with Bogen magnetic tape affixed to groove in encoder disk

A mounting bracket was fabricated to mount two encoder read heads a precise distance away from the encoder disk. Two encoder read heads were utilized in order to cancel out errors due to encoder disk non-concentricity and swash (Renishaw, 2009). Use of multiple read heads is standard practice in professional telescopes (Mancini et al, 1998). For the magnetic encoder used in this project, the Renishaw/RLS LM10IC (RLS, 2011), the read head ride height above the tape must be maintained to within 0.7mm to achieve optimal accuracy.

The *sub-divisional error* (otherwise known as *interpolation error*) of the encoder increases rapidly if the gap between the magnetic tape and read head is increased – for a 2mm pole path magnetic tape, the SDE is +/- 3.5μm for ride heights below 0.7mm but increases to +/- 7.5μm at a ride height of 1mm (RLS, 2011). The diameter of the encoder disk imposes a limit on the accuracy of encoder – since the length of the magnetic tape is 910mm, the SDE is +/- 5” at ride heights below 0.7mm and +/- 11” at a ride height of 1mm. The accuracy of the system can be increased (and sub-divisional error decreased) by using a larger encoder disk. However, such an approach was not practical for this project; the 290mm disk was already impracticably large for use in the field.

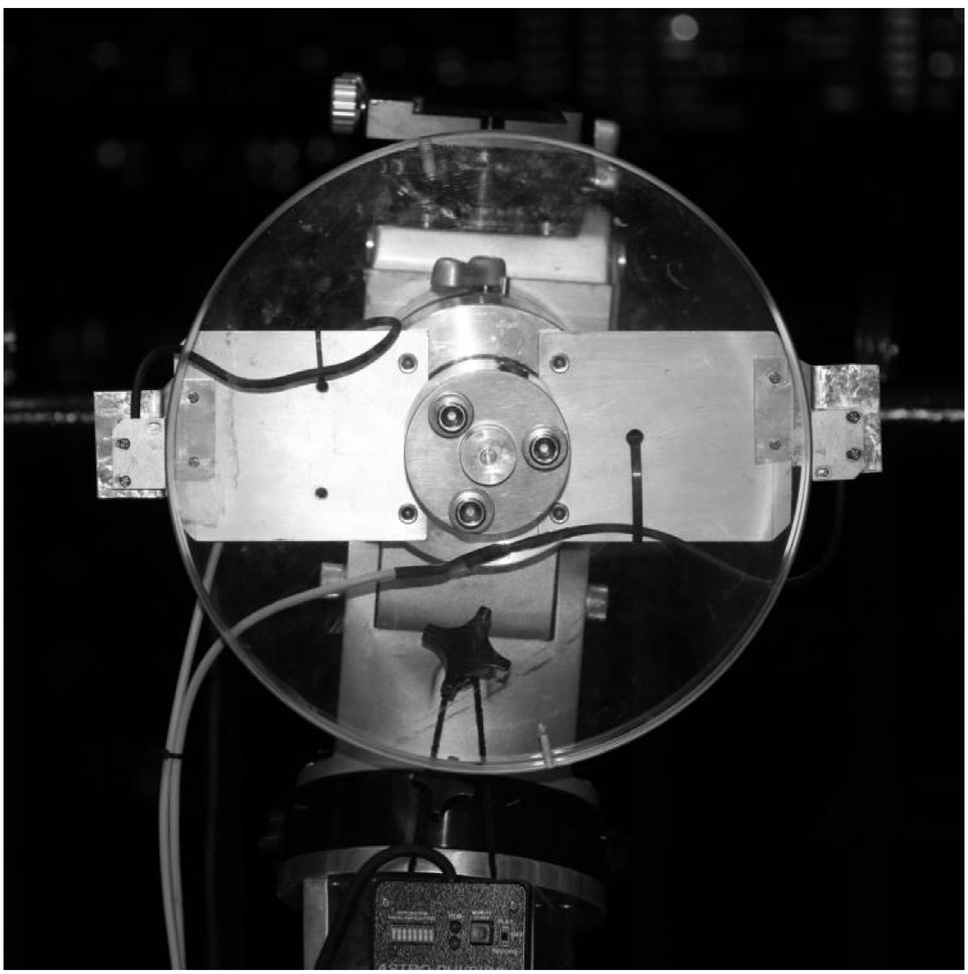

Fig. 3. Perpendicular view of encoder disk, mounting brackets for encoder read heads, and two read heads at 3- and 9 o’clock

The LM10IC encoders generated RS-422 (differential digital) signals in quadrature – an A channel (with A+ and A- signals) and a B channel (with B+ and B- signals) (RLS, 2011). These digital signals were internally generated using an uncorrected arc-tangent algorithm within the LM10IC read head (Cvetkovic, 2013, personal communication). 2000 positions were interpolated in-between each pole pair on the magnetic tape (of 2mm pole length), resulting in a resolution of 1μm per quadrature tick (RLS, 2011).

The differential digital signals were converted to normal digital signals using 75157 dual-differential line receivers (Texas Instruments, 1997). Because each encoder had an A and B signal, two 75157's were required. The digital A and B signal outputs of each encoder were routed to the interrupt-capable pins (pins 18, 19, 20, and 21) (IWeb) of an Arduino Mega1280 microcontroller (AWeb). An Arduino Mega1280 processor was used because it has four hardware interrupt pins – pins 18, 19, 20, and 21 – ensuring that encoder ticks were not lost when the mount is rapidly moved (IWeb). The encoder counts were maintained using the PJRC Encoder Library (EWeb), which significantly simplified the task of handling the encoder interrupt routines.

The encoder counts for each encoder were stored as long integers within the memory of the Atmel processor in the Arduino. At any given time, the time from boot of the Arduino was provided by the *millis()* function – and thus the theoretical encoder angle could be determined by multiplying the *millis()* value by the sidereal rate of 15.036"/second. The error or deviation from the theoretical encoder angle for the two encoders was simply the difference between the encoder count of each encoder, and the theoretical angle. These errors drifted over time due to mechanical misalignment, but by averaging the two errors, a corrected value could be obtained.

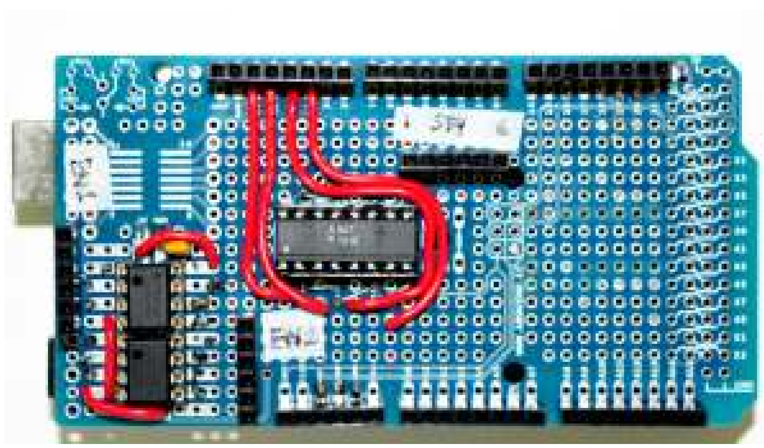

Fig. 4. Encoder electronics (2x 75157 differential line receivers at bottom-left, 1x ACPL847 optocoupler in center)

Ideal signals from encoders are a pair of sinusoids with a quadrature phase difference between them – in other words, the A channel signal is a sine, and the B channel signal is a cosine. Interpolation operates on the relative difference in amplitude and phase of these paired sinusoids by calculating the arc-tangent of the A and B signals. Therefore, interpolation errors will occur if the pair-periodic signals deviate from the ideal waveforms (Tan et al, 2002). The mechanism used to compensate the mean value (offset) errors, phase, and amplitude errors for two quadrature sinusoidal signals was first described by Heydemann (1981) who employed least-squares fitting to compensate for non-ideal analog quadrature signals. The Gemini telescope utilized Heydemann correction on its encoder system (Fisher and Wilkes, 1997). This type of correction is not done in the Renishaw/RLS LM10IC encoder (Cvetkovic, 2013) due to cost and computational complexity limits, resulting in substantial sub-divisional error.

Because the LM10IC performs interpolation internally and does not output analog quadrature signals – a related product, the LM10AV, *does* output analog quadrature, but was not available for this project – it was not possible to use Heydemann interpolation or similar techniques such as the adaptive learning algorithm of Kavanagh (2001) to correct the sub-divisional or interpolation errors.

The 189-second period of the SDE is derived from the pole length of 2mm and the sidereal rate – which is 15.036"/second (average). Due to the 290mm diameter of the encoder disk, the resolution is 1.424"/μm. The 2mm pole path (2000μm which corresponds to 2848") is thus traversed in approximately 189.4 seconds.

It is possible to exploit the periodic nature of the sub-divisional error using two encoders. The SDE of each encoder is roughly a sinusoid with a period equal to the magnetic tape pole length (2mm) with lesser-amplitude components at higher frequencies (Cvetkovic, 2013). In the following figure, the raw periodic error of the mount (green line) was reported at +/- 9" – however this raw error was actually the sum of the mount's mechanical periodic error, and the +/- 5" sub-divisional error of the encoder itself. The sinusoid with a period of 449 seconds was the mechanical periodic error of the mount, while the fast sinusoid with a 189-second period was the fundamental frequency of the sub-divisional error. Hence the mount's actual periodic error was about 8" to 10" peak-to-peak, as verified through independent measurement using PEMPro software (Gralak, 2013).

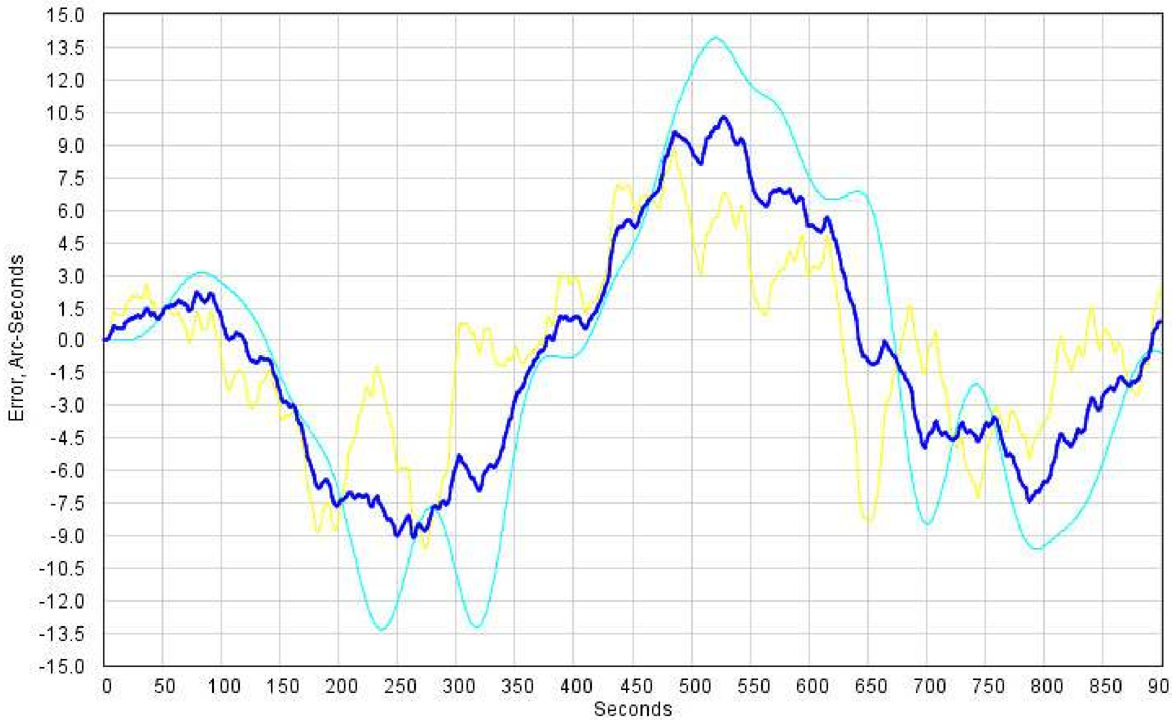

Fig. 5. Measured periodic error of mount, showing both mount periodic errors and interpolation/sub-divisional error

If the two encoders are precisely offset at opposing sides of the encoder wheel (e.g. by 1mm) it would be possible for the SDE of the two encoders to precisely cancel each other out. This would however require precise calibration of the encoder mountings. An alternative method is to phase-shift in time (temporally-shift) the output of one encoder with respect to the other until a perfect 180 electrical degree phase-shift is obtained for the 189-second SDE fundamental. This would allow the SDE to be canceled without requiring rigorous mechanical calibration of the encoder read heads.

In this project, a least-squares algorithm was used to calculate the temporal offset between the two encoders that resulted in the **maximum** sum of squares between the two encoder counts. Intuitively, the sum of squares is maximum when the SDE of the two encoders are perfectly out of phase (and hence ideal for cancelling each other out).

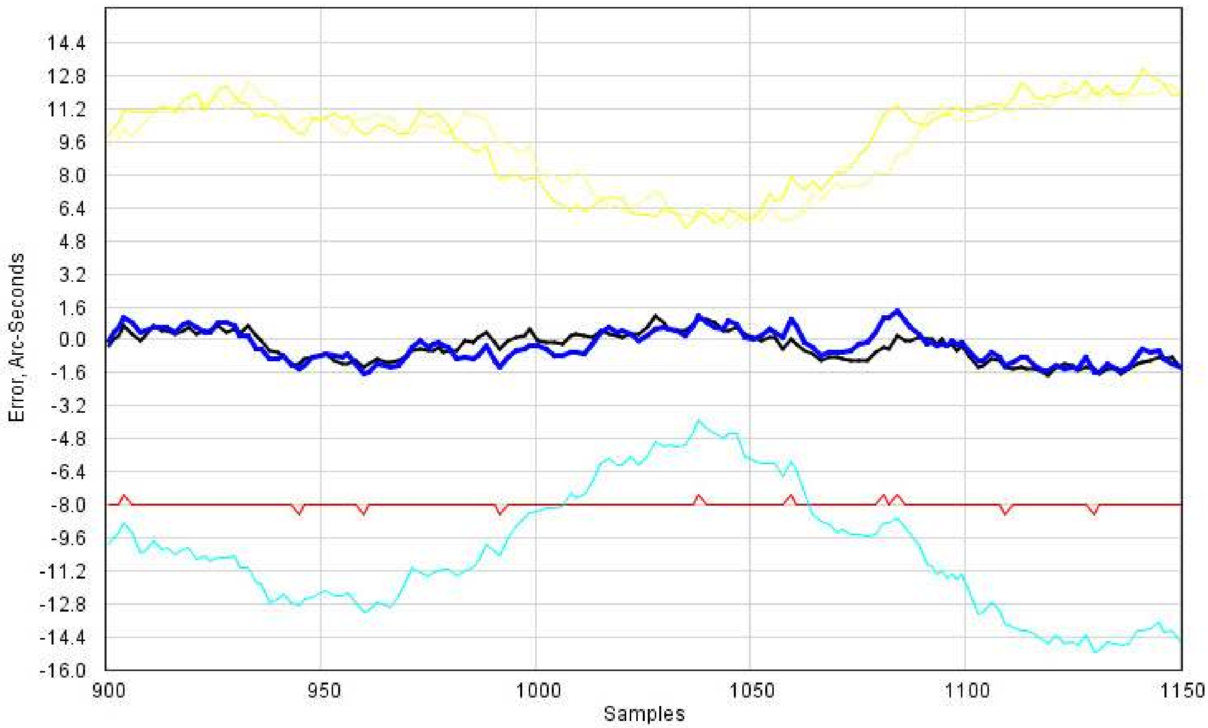

Fig. 6. Residual error from encoder A and B after correction, and averaged encoder error

In the figure above, the horizontal scale was samples of 0.5 seconds each. Hence the encoder A and B signals (uppermost and lowermost traces) were sinusoids with period of 189 seconds. These sinusoids were not the mount periodic error because the mount periodic error had a 449-second period (due to the 192 teeth on the mount worm). The amplitude of the SDE is observed to be about about 10" – in perfect agreement with the LM10IC data sheet specification of +/- 3.5μm (+/- 5").

The central trace in Figure 5 was the corrected encoder signal, after averaging the encoder A and B signals. The long-term drift of each encoder (due to mechanical fabrication inaccuracies) and the encoder SDE were both satisfactorily canceled, with a residual error of approximately +/- 1.6". During multiple trials, it was determined that the maximization of the sum-of-squares algorithm only operated successfully if the two encoders were (nearly) 180 electrical degrees out of phase – hence mechanically adjusting the encoders was still required, although the requirement of perfect mechanical offset was related. The upper trace shows both the original encoder data and the temporally-shifted data from the sum-of-squares algorithm. The temporal shift was very minimal, indicating that the encoders were satisfactorily aligned mechanically.

After determination of the encoder error attributable to the mount periodic error (after processing the signals to eliminate systematic errors) the necessary guide pulse length to correct this error could be calculated. At a guide speed of 1X sidereal, a 1-second pulse would cause a movement of 15.036" approximately. Hence if at any given time an error of 5" were calculated, a guide pulse in the opposite direction of (5 / 15.036) = 330ms would be required to correct such error. In practice, a shorter pulse length was used to prevent instability of the servo loop and mechanical overshoot, since the mount does not respond instantaneously to guide corrections. The Arduino microcontroller provided feedback to the mount through the ST-4 guide port. An optical isolator (ACPL 847) was used to electrically isolate the Arduino electronics from the mount electronics (Avago Technologies, 2008).

It was also determined during experimentation that the King rate and refraction-corrected tracking rate did not significantly alter the accuracy of encoder tracking due to the magnitude of the encoder SDE, hence variable-rate tracking was not implemented.

The full schematic diagram for the Arduino and interface electronics from the encoder and to the mount is described in the Appendices.

Equipment

Long-exposure (600-second) images of star fields were obtained using an Astro-Tech AT90EDT triplet apochromatic refractor, with an Orion non-reducing flattener, a Santa Barbara Instruments Group ST8300M monochrome CCD camera, and a non-GoTo Astro-Physics 600E Quartz Micro Drive mount. The pixel scale was 1.86” per pixel with this setup. Exposures were taken through a Baader 2” 7nm hydrogen-alpha filter to allow long exposures; without the filter the CCD camera would saturate due to sky glow in less than 2 minutes.

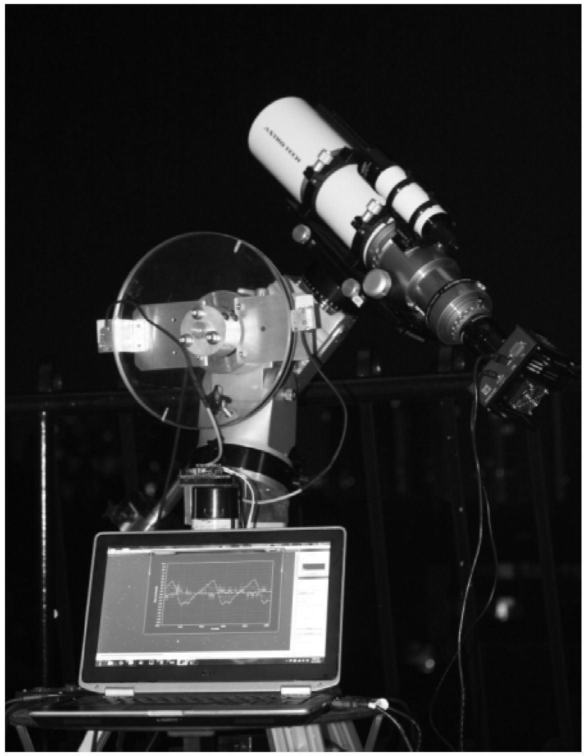

Fig. 7. Observational setup while making exposures

To determine the effectiveness of the encoder correction system, a number of 10-second and 600-second exposures were taken. The 10-second exposures were used to characterize the seeing and to estimate how good the focusing was, since no automatic focusing routine was available. The rationale was that 10-second exposures would show no mount errors, and thus only reflect the quality of the seeing and focusing.

600-second exposures were taken with and without the encoder enabled. The Full Width Half Maximum (FWHM) of stars in the images was calculated using Deep Sky Stacker software (Coiffier, 2011). In addition, to serve as a reference, five guided 600-second images taken from New Mexico with the Global Rent-A-Scope system in 2011 were also used for comparison. These images were taken with an SBIG ST8300C (the color version of the CCD used in this project), Takahashi FSQ-106ED 106mm quadruplet refractor, and Paramount ME mount. The pixel scale for the GRAS images was 2.1”/pixel. The Bayer matrix did not significantly reduce empirical FWHM for mid-temperature (white) stars so a direct angular FWHM comparison could be done (Moore, 2013, personal communication).

Data Reduction

The observational details and results were as follows:

Observation Date	11:20pm SGT 28 October 2013 – 01:20am SGT 29 October 2013		**Target Coordinates**	RA 23h 04m 26s DEC 28° 11' 26"
Exposure Time	**# of Samples**	**Average FWHM**	**Minimum FWHM**	**Maximum FWHM**
10s	20	6.73”	6.44”	7.20”
600s unguided	112	7.23”	6.77”	7.70”
	04:57 – 05:17am SGT 1 November 2013			RA 04h 27m 45s DEC 22° 42' 14"
10s	20	6.78”	5.51”	7.86”
600s unguided	3	7.28”	6.85”	7.53”
	05:31 – 06:00 am 1 November 2013			RA 04h 27m 52s DEC 22° 41' 34"
600s encoder	5	7.14	6.79	7.81
	03:32 – 04:33 am 2 November 2013			RA 02h 50m 00s DEC 27° 00' 18"
10s	20	4.78	4.18	5.05
600s encoder	6	6.79	5.98	7.07
	09:48 – 10:28 pm 4 November 2013			RA 19h 31m 00s DEC 21° 56' 00"
10s	6	5.49”	4.90”	6.38”
600s unguided	6	7.29”	6.35”	7.94”
	02:51 – 03:42 am 5 November 2013			RA 02h 51m 00s DEC 34° 44' 00"
600s encoder	6	7.08”	6.86”	7.46”
Reference Images				
600s guided	5	6.80”	6.24”	7.56”

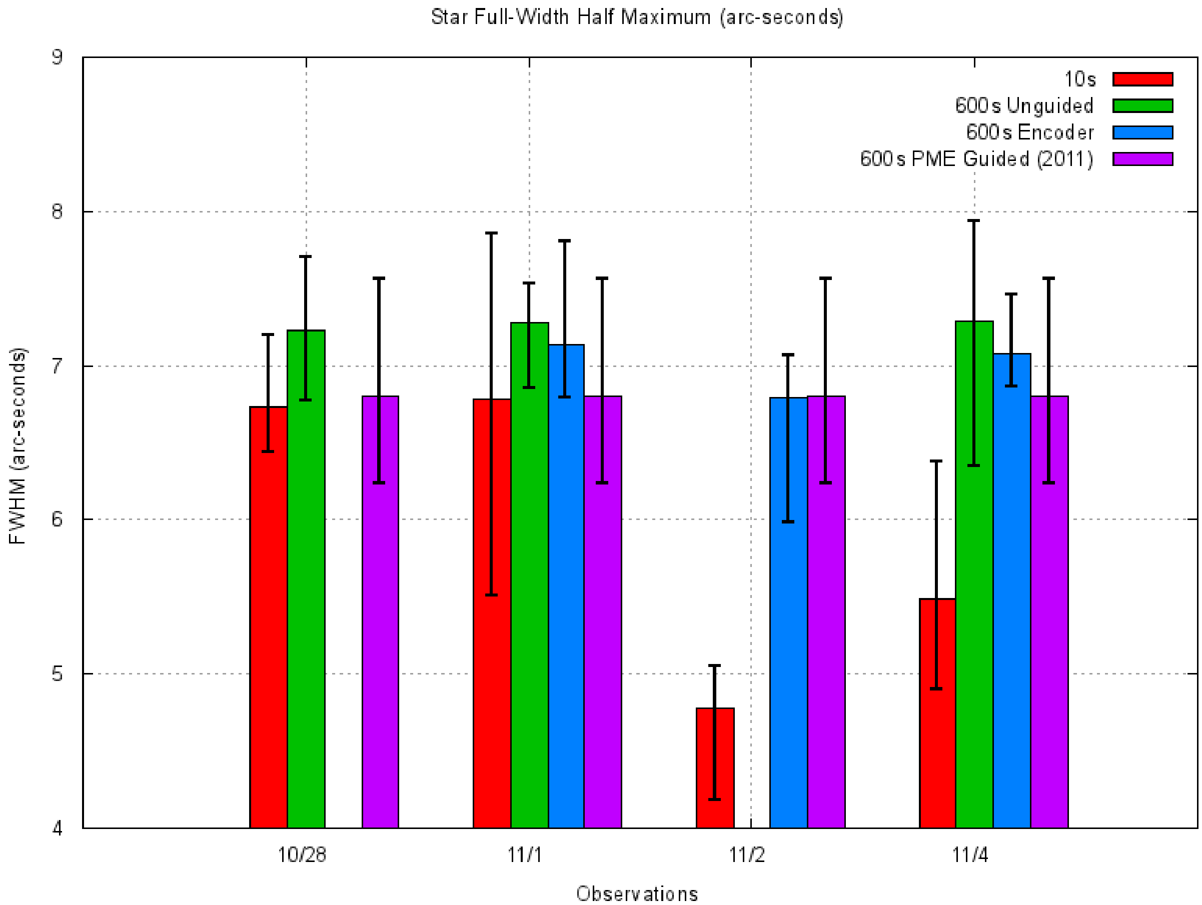

Fig. 8. Experimental results

Star Full-Width Half Maximum for 10-second exposures on 11 November was significantly lower than on other observation dates, possibly due to favorable atmospheric conditions. Focusing accuracy was consistent for all observation dates, as real-time CCD FWHM minimization was used for focusing manually.

A two-tailed unpaired T-test was used to compare the 600-second unguided, encoder-corrected, and GRAS guided images. Data for all 600-second exposures were as follows:

	600s	600s Encoder	GRAS
	6.77	6.79	6.237
	6.79	6.97	6.741
	6.86	7.05	6.363
	7.01	7.09	7.119
	7.23	7.81	7.56
	7.25	5.98	
	7.29	6.79	
	7.36	6.85	
	7.42	7.03	
	7.49	7.03	
	7.53	7.07	
	7.70	6.86	
	6.85	6.90	
	7.46	6.97	
	7.53	7.10	
	6.35	7.18	
	6.99	7.46	
	7.20		
	7.60		
	7.66		
	7.94		
Average	7.25	7.00	6.80
Standard Deviation	0.38	0.36	0.55
T-Test		0.043	0.494

Mean Full-Width Half Maximum for 600-second unguided exposures was 7.25”; FWHM for encoder-corrected images was 7.00”; and FWHM for GRAS Paramount ME guided exposures was 6.80”. There was a statistically significant difference between the FWHM of unguided and encoder-corrected images ($p = 0.043$) at the 5% confidence level.

There was no significant difference between the FWHM of encoder-corrected image and guided images on a Paramount ME in New Mexico ($p = 0.494$) at the 5% confidence level.

Sources of Errors

The most significant source of errors in the encoder system was the encoder sub-divisional error of +/- 5”. This SDE was actually equal to in magnitude or larger than the mechanical periodic error of the mount of about 8” to 10” peak-to-peak. Furthermore, the SDE period of 189 seconds was faster than the mount period of 449 seconds; hence the instantaneous error velocity for the SDE was about a factor of 3 higher. Hence, SDE correction was absolutely essential – the encoder solution is worthless if SDE was not reduced.

The second source of errors was polar misalignment. Polar alignment of only approximately 8’ from the pole was achieved; hence declination drift elongated stars in the north-south direction, increasing the FWHM of stars in both guided and encoder-corrected exposures, since both approaches could not take declination drift into account.

A third source of errors was enlarged star FWHM due to the inadequate pixel scale of 1.86”/pixel. With such a pixel scale, a 6” FWHM star would only span 3-4 pixels, and FWHM calculation algorithms break down with such small stars (Moore, 2013, personal communication). This error was evident both on exposures taken during the course of this project, and exposures taken in New Mexico in 2011.

Atmospheric seeing and haze, quantified by FWHM in the 10-second exposures, was not a factor in the 600-second exposures. As there was no statistically significant difference in the 600-second encoder-corrected exposures and the New Mexico images (New Mexico enjoys 2” to 3” seeing and cloudless nights) this showed that atmospheric conditions did not contribute significantly to stellar FWHM on long exposures at this pixel scale.

A final and potentially important source of errors was the limited number of exposures, particularly for the encoder-corrected and New Mexico guided images. A larger number of exposures would provide more rigorous statistical verification of the effectiveness of the encoder solution.

Conclusion

The use of low-cost multiple encoders with limited resolution and significant sub-divisional error was effective in reducing the Full-Width Half Maximum size of stars in 600-second unguided exposures. Algorithms for correcting sub-divisional error and mechanical misalignments proved successful. Such a solution would provide even greater benefits on less-precise mounts (the Astro-Physics 600E QMD mount used in this project had a peak-to-peak mechanical periodic error of about 8” to 10”, as compared to the 25” to 40” periodic error of many mass-produced Chinese equatorial mounts).

Fig. 9. Comparison of unguided (left) and encoder-corrected (right) images

However, the excessively large encoder disk of 290mm diameter limited the usefulness of this prototype for field use; and a smaller disk would have insufficient accuracy. Therefore, encoders with a resolution finer than 1μm are necessary for a field-usable solution.

References

Covington, Michael A. "Astrophotography for the Amateur", Cambridge University Press, 2nd ed. 1999.

Reid, I.N.; Brewer, C.; Brucato, R.J.; McKinley, W.R.; Maury, A.; Mendenhall, D.; Mould, J.R.; Mueller, J.; Neugebauer, G.; Phinney, J.; Sargent, W.L.W.; Schombert, J.; and R. Thicksten. "*The Second Palomar Sky Survey*," Publications of the Astronomical Society of the Pacific, 103: 661-674, July 1991.

Colon, K.D. and E. Gaidos, "Narrow-K-Band Observations of the GJ 1214 System," arXiv:1308.4404, 2013.

Encoder Tests, Gemini Mount Control System Report, MCSJDW11 (Issue 1), 10 July 1996

Ulich, B., Montgomery, J., Poyner, A. & Janes, C. "*Correcting Periodic Error in Telescope Absolute Encoders*," MMTO Tech Memo 84-17, 11 June 1984.

C. S. Amos, J. E. Churchill, M. Fisher, R. A. Laing. "*William Herschel Telescope Inductosyn Tape Encoder Project*," September 1992. RGO Report - RGO-N-008.

M. Fisher, "*A High Resolution Incremental Tape Encoder On The William Herschel Telescope*," Advanced Technology Optical Telescopes V, SPIE Vol. 2199, March 1994.

F. Ruhle, "*Comments on Report RGO-N-008 - William Herschel Telescope Project,*" Inductosyn International. EN7032. January 1996.

M. Fisher & J. Wilkes, "*Encoder Considerations,*" Gemini Mount Control System Report, November 1995.

J. Wilkes & M. Fisher, "*Selection of a tape encoding system for the main axis of the Gemini telescopes*," Proc. SPIE 3112, Telescope Control Systems II, 30 (September 18, 1997); doi:10.1117/12.278836, From Conference Volume 3112, in Telescope Control Systems II, ed. Hilton Lewis, July 27, 1997

Erm, T. & Sandrock, S. "*Adaptive periodic error correction for the VLT telescopes,*" Proc. SPIE Large Ground-Based Telescopes, Vol. 4837-106, 2002

Erm, T. & Sandrock, S. "*Adaptive Correction of Periodic Errors Improves Telescope Performance*," 2005 American Control Conference, 8-10 June 2005

Yang, Y., Rees, N. P., & Chuter, T., "*Application of a Kalman Filter at UKIRT,*" Astronomical Data Analysis Software and Systems IX, ASP Conference Proceedings, Vol. 216, edited by Nadine Manset, Christian Veillet, and Dennis Crabtree. Astronomical Society of the Pacific, ISBN 1-58381-047-1, 2000., p.279

Lambermont, H. "*An astrophotography mount performance overview,*" http://lambermont.dyndns.org/astro/pe.html (retrieved 14 September 2013)

Explore Scientific, "*Telescope Drive Master,*" http://www.explorescientific.com/telescopedrivemaster/ (retrieved 14 September 2013)

Vanleenhove, M. "*A heavy, easy to move mount: the Gemini-41,*" http://www.supernovae.be/review_g41 (retrieved 17 September 2013)

HWeb: "*Ultra-Precise Positioning of the Largest Telescope in the Northern Hemisphere by HEIDENHAIN,*" http://news.thomasnet.com/companystory/Ultra-Precise-Positioning-of-the-Largest-Telescope-in-the-Northern-Hemisphere-by-HEIDENHAIN-822798, 2008 (retrieved 15 November 2013)

Renishaw plc, "*The Accuracy of Angle Encoders,*" http://resources.renishaw.com/en/download/white-paper-the-accuracy-of-angle-encoders--24170, 2009.

Bogen Electronic, "*Datasheet Magnetic Tape,*" http://www.bogen-electronic.com/tl_files/pdf/Datenblatt_Magnetband_Ausg_d.pdf (retrieved 15 November 2013)

RLS merilna tehnika d.o.o., "*LM10 linear magnetic encoder system data sheet,*" LM10D01_11, Issue 11, 5th May 2011

Cvetkovic, B., RLS merilna tehnika d.o.o., personal communication, 24 September 2013

Heydemann, P. L. M., "*Determination and correction of quadrature fringe measurement errors in interferometers,*" Applied Optics, Vol. 20 No. 19, 1 October 1981.

Mancini, D., Auricchio, A., Brescia, M., Cascone, E., Cortecchia, F., Schipani, P., and G. Spirito, "*Encoder system design: strategies for error compensation*," Astronomical Observatory of Capodimonte - Technology Working Group (TWG), 1998

Tan, K.K., Zhou, H.X., & Lee, T.H. "*New Interpolation Method for Quadrature Encoder Signals,*" IEEE Transactions on Instrumentation and Measurement, Vol. 51, No. 5, October 2002

Kavanagh, R.C. "*Probabilistic Learning Technique for Improved Accuracy of Sinusoidal Encoders,*" IEEE Transactions on Industrial Electronics, Vol. 48, No. 3, June 2001

Texas Instruments, "*SN75157 Dual Differential Line Receiver,*" SLLS084C – September 1980 – Revised March 1997

Avago Technologies, "*ACPL-8x7 Multi-Channel Full-Pitch Phototransistor Optocoupler Data Sheet,*" AV02-1429EN - December 22, 2008

AWeb: "*Arduino Mega,"* http://arduino.cc/en/Main/arduinoBoardMega (retrieved 15 November 2013)

IWeb: "*attachInterrupt,*" http://arduino.cc/en/Reference/attachInterrupt (retrieved 15 November 2013)

EWeb: "*Encoder Library,*" http://www.pjrc.com/teensy/td_libs_Encoder.html (retrieved 15 November 2013)

Gralak, R. "*PEMPro V2*," http://www.ccdware.com/products/pempro/ (retrieved 16 November 2013)

Coiffier, L. "*Deep Sky Stacker,*" http://deepskystacker.free.fr (retrieved 3 Dec 2011).

Moore, S. contributing author to "*Lessons from the Masters: Current Concepts in Astronomical Image Processing,*" The Patrick Moore Practical Astronomy Series, Vol. 179, 2013. Personal communication, 8 November 2013.

Appendices